

Excerpt of Dr. Edgar J. Gunter's interview about Melvin Prohl, the "father of modern rotordynamics," in 2018.

Question. What is the significance of this paper, "A General Method for Calculating Critical Speeds of Flexible Rotors"?

Edgar J Gunter. This paper was written in 1945 by Melvin Prohl. It marks the development of the transfer matrix method—and beginning of modern rotor dynamics.

Q. What was so important about the transfer matrix method?

EJG. It was the first time that engineers could compute critical speeds with greater accuracy and simplicity. Back in 2008 at one of my training courses, we used Dyrobes to recreate the analysis in the paper. We found that Prohl's results in the original paper were very accurate.



Q. How did Prohl come up with such accurate results without a modern rotor dynamics computer program?

EJG. Many years ago, while in Texas at the Turbo conference, I had a chance to sit down with him over a few beers. He told me that back then he had three teams of women working on Marchant mechanical calculators to crunch the numbers. I asked him if they all got the same results. "No," he said. "I usually averaged them!"

Q. How did modern computers affect rotor dynamic analysis?

EJG. Jorgen Lund, who worked for Prohl, programmed the transfer matrix method in Fortran on their new 360 IBM units. Lund later expanded the transfer matrix method for unbalance response and stability.

Q. Why is the transfer matrix method no longer the industry standard?

EJG. The transfer matrix method breaks down with multiple bearings and supports. Back in the 70s, when I was researching the dynamics of the 1150 MW nuclear turbine-generator with 11 bearings, my advanced transfer-matrix-based critical-speed program missed modes.

Q. Did you get better results from a Finite Element Analysis code?

EJG. Not at the time. The 11 or 12 system modes were computed by the MSC Pal finite element program. The problem with this, and all finite element codes at that time, is that they were based on having symmetrical system matrices. Hence they can't handle bearings, stability (damped eigenvalue analysis) on unbalance response.

Q. When did you begin using FEA instead of your own advanced transfer matrix analysis?

EJG. For me, it was when Wen Jeng (Dr. Wen Jeng Chen) showed that Dyrobes could compute all the modes for the 1150 Mega Watt Turbine Generator system including foundation effects using finite element methods. He was working with Dr. Harold Nelson who used unsymmetric matrices which allow you to compute fluid film bearings and gyroscopic effects. In fact, Melvin Prohl said that it was essential to have proper computations of higher modes for their turbine development. I'm sure Prohl would be very pleased to see the advancement in rotor dynamics, especially the accomplishments of Dyrobes to perform nonlinear time transient computations of turbochargers.

A General Method for Calculating Critical Speeds of Flexible Rotors

By M. A. PROHL,¹ WEST LYNN, MASS.

The existing methods for determining critical speeds are subject to the following limitations: On the one hand the methods that are general, i.e., that permit the calculation of higher critical speeds as well as the fundamental, involve computations so complicated as to be impractical for any but the simplest of rotors. On the other hand, the methods for which the computations are comparatively simple, such as the familiar methods of Rayleigh and Stodola, lack generality in that critical speeds other than the fundamental cannot be definitely determined (1).² The calculation method presented in this paper combines generality with comparative simplicity. Any critical speed—first, second, or higher—may be calculated with equal ease. The rotor may have any number of spans and its cross section may vary in any prescribed manner provided circular symmetry is maintained. Any number of disks or symmetrical masses may be attached. The shaft journals may be considered to be elastically supported in the bearing with respect to both deflection and tilting of the journals; the elastic constant must, however, be symmetrical. The so-called "microscopic effect" associated with the moment of inertia of the disks on the rotor may be readily taken into account.

NOMENCLATURE

The following nomenclature is used in the paper:

- A = mass moment of inertia of disk about its axis of symmetry, lb-in-sec²
- B = mass moment of inertia of disk about axis through center of gravity and normal to axis of symmetry, lb-in-sec²
- C = bearing stiffness factor for resistance to tilting of shaft, lb-in.
- D = diameter of disk, in.
- E = modulus of elasticity, psi
- H = angular momentum, lb-in-sec
- h = thickness of disk, in.
- I = diametral moment of inertia of shaft cross section, in.⁴
- K = bearing stiffness factor for resistance to deflection of shaft, lb per in.
- M = bending moment, lb-in.
- m = mass, lb-sec²/in.
- t = time, sec
- V = shearing force, lb
- x = distance along shaft, in.

¹ Turbine Engineering Division, General Electric Company. Jun. A.S.M.E.

² Numbers in parentheses refer to the Bibliography at the end of the paper.

Contributed by the Applied Mechanics Division and presented at the Annual Meeting, New York, N. Y., Nov. 27-Dec. 1, 1944, of THE AMERICAN SOCIETY OF MECHANICAL ENGINEERS.

Discussion of this paper should be addressed to the Secretary, A.S.M.E., 29 West 39th Street, New York, N. Y., and will be accepted until Oct. 10, 1945, for publication at a later date. Discussion received after the closing date will be returned.

NOTE: Statements and opinions advanced in papers are to be understood as individual expressions of their authors and not those of the Society.

- y = deflection of shaft, in...
- β = shaft-section flexibility constant (1/lb-in.)
- θ = slope of shaft (nondimensional)
- μ = mass per unit length, lb-sec²/in.³
- ρ = mass density lb-sec²/in.⁴
- ϕ = angle, radians
- ω = speed of rotation or frequency of vibration, radians per sec

GENERAL CONSIDERATIONS

For a balanced shaft of variable diameter which is rotating or "whirling" steadily at a critical speed ω with its central axis in a bowed shape, the following differential equation applies (2, 3)

$$\frac{d^2}{dx^2} \left(EI \frac{d^2 y}{dx^2} \right) = \mu \omega^2 y \dots \dots \dots [1]$$

From the elementary beam theory

$$EI \frac{d^2 y}{dx^2} = M \dots \dots \dots [2]$$

Equation [1] becomes

$$\frac{d^2 M}{dx^2} = \mu \omega^2 y \dots \dots \dots [3]$$

Equation [1] is a fourth-order differential equation, and hence there are four boundary conditions to be satisfied. Any speed of rotation for which it is possible to effect a solution of this equation which satisfies these four boundary conditions constitutes a critical speed. Equations [2] and [3] form the basis for making such a solution by a simultaneous construction of the bending-moment and deflection diagrams using a step-by-step integration process. Let the shaft be divided into a series of appropriate sections. Equations [2] and [3] may be rewritten as follows

$$\Delta \left(\frac{dy}{dx} \right) = \left(\frac{\Delta x}{EI} \right) M_{avg} \dots \dots \dots [4]$$

$$\Delta \left(\frac{dM}{dx} \right) = (\mu \omega^2 \Delta x) y_{avg} \dots \dots \dots [5]$$

where Δx is the length of a given section and M_{avg} and y_{avg} are the average values of bending moment and deflection for that section.

Equation [4] states that the change in slope of the deflection curve which occurs at the given section is proportional to the average bending moment, the proportionality factor being the flexibility constant $\left(\frac{\Delta x}{EI} \right)$. Equation [5] states that the change in slope of the bending-moment diagram, which occurs at the given section, is proportional to the average deflection, the proportionality factor being the inertia force of the section mass per unit of deflection $(\mu \omega^2 \Delta x)$.

Dr. H. Poritsky of the Engineering General Division of the author's company has proposed a graphical method of solution in which the bending moment and deflection diagrams are represented by a series of straight-line segments; the finite changes in

slope between adjacent segments being given by Equations [4] and [5].

The calculation method presented in this paper is on a numerical rather than a graphical basis, and the integration procedure is somewhat more elaborate than that indicated in the foregoing equations. A tabular form has been prepared to assist the calculator.

In general, for any assumed speed of rotation, bending-moment and deflection diagrams can be constructed which satisfy three of the four required boundary conditions. Only if the assumed speed of rotation is exactly equal to a critical speed can the fourth boundary condition also be satisfied. Hence by plotting the discrepancy in the fourth boundary condition as a function of the assumed speed, and noting where the discrepancy becomes zero, the various critical speeds can be obtained. In plotting such a curve, it is necessary to select some arbitrary boundary condition and hold it constant. Such a condition might be, for example, the slope of the deflection curve at a shaft end simply supported in a bearing.

The numerical method of this paper is analogous to Holzer's method (4) for calculating natural frequencies of torsional vibration. However, the problem of calculating critical speeds is inherently more complicated since four integrations are involved instead of two, and additional complications arise in dealing with the boundary conditions.

It should be noted that the foregoing type of analysis applies equally well to the determination of the natural frequencies of transverse vibration of a beam of variable cross section since Equation [1] is also the differential equation for this case.²

THE CALCULATION METHOD

In order to apply the numerical-calculation method of this paper, the actual rotor must be transformed into an idealized equivalent system consisting of a series of disks connected by sections of elastic but massless shaft. The mass of these disks and their spacing are chosen so as to approximate the distribution of mass in the actual rotor. Likewise, the bending flexibility of the connecting sections of shaft is taken so as to correspond to the actual flexibility of the rotor. In the discussion which immediately follows, it will be assumed that the moment of inertia of the disks is negligible so that the disks may be treated as mass points.

In Fig. 1, a portion of an idealized system is shown together with the shearing force, bending moment, and deflection diagrams. Assume that this system is whirling in the deflected position at some speed ω . Since each section of shaft is massless, the shearing force is constant between any two masses, and hence the bending-moment diagram has a constant slope directly equal to the shearing force (5)

$$\frac{dM}{dx} = V \dots \dots \dots [6]$$

A finite change in shearing force occurs at each mass, which is equal to the inertia force of the mass

$$\Delta V = m\omega^2 y \dots \dots \dots [7]$$

This finite change in shearing force results in a finite change in slope of the moment diagram at each mass. Because of the continuity of the shaft, the deflection diagram is a smooth curve with no breaks or discontinuities. The equation for the variable slope

² After this paper had been submitted, the author's attention was drawn to a recently published paper by N. O. Myklestad in which a method for calculating natural frequencies of transverse beam vibration is presented that is fundamentally the same as the method of this paper although quite different in its application. See reference (6) in the Bibliography.

of the deflection curve for each section will be a quadratic, and the equation for the deflection curve will be a cubic.

Assume that the following quantities are known at the left-hand end of the system in Fig. 1:

- V_0 = shearing force (due to bearing reaction)
- M_0 = bending moment (due to bearing reaction)
- θ_0 = slope of deflection curve
- y_0 = deflection

There will be a change in shearing force at point 0 due to the inertia force of the mass m_0 according to Equation [7], and hence the shearing force V_1 for the section of shaft between point 0 and point 1 (section 1) is

$$V_1 = V_0 + m_0\omega^2 y_0 \dots \dots \dots [8]$$

The bending moment M_1 at point 1 is

$$-M_1 = M_0 + V_1(\Delta x)_1 \dots \dots \dots [9]$$

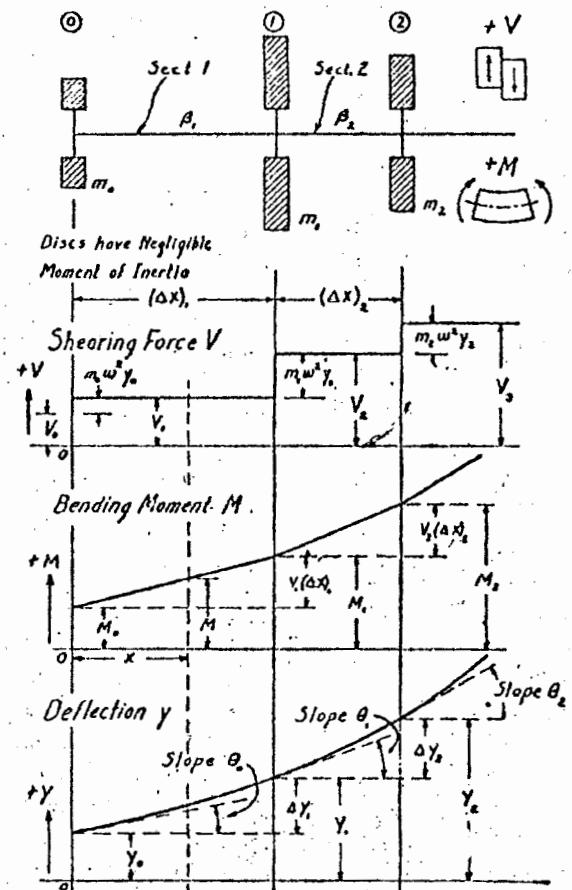


FIG. 1 SHEARING-FORCE, BENDING-MOMENT, AND DEFLECTION DIAGRAMS FOR AN IDEALIZED SYSTEM

The bending moment M at any distance x from the left-hand end of section 1 is

$$M = M_0 + \frac{V_1 - M_0}{(\Delta x)_1} x \dots \dots \dots [10]$$

The slope θ of the deflection diagram for the first section is obtained as follows

$$\theta = \frac{1}{(EI)} \int_0^x M dx + c \dots \dots \dots [11]$$

where c is a constant of integration. Substituting Equation [10] into [11] and integrating from the top down to the point of interest, the following equations are

The deflection y is obtained as follows

$$y = \int_0^x \theta dx + c' \dots \dots \dots [13]$$

where c' is a constant of integration.

Substituting Equation [12] in [13] and integrating gives

$$y = \frac{1}{(EI)_1} \left[M_0 \frac{x^2}{2} + \frac{M_1 - M_0}{(\Delta x)_1} \frac{x^3}{6} \right] + \theta_0 x + y_0 \dots [14]$$

It is only necessary to know the slope θ and the deflection y at the end of the section (i.e., point 1). Substituting $(\Delta x)_1$ for x and β_1 for $\left(\frac{\Delta x}{EI}\right)_1$ in Equations [12] and [14] gives

$$\theta_1 = \beta_1 \left(\frac{M_0}{2} + \frac{M_1}{2} \right) + \theta_0 \dots \dots \dots [15]$$

$$y_1 = \beta_1 \left(\frac{M_0}{3} + \frac{M_1}{6} \right) (\Delta x)_1 + \theta_0 (\Delta x)_1 + y_0 \dots \dots [16]$$

From the value of the deflection at point 1, as given by Equation [16], it is now possible to evaluate the change in shearing force at point 1, and hence the shearing force V_2 in shaft section 2.

$$V_2 = V_1 + m_1 \omega^2 y_1 \dots \dots \dots [17]$$

The bending moment M_2 at point 2 is

$$M_2 = M_1 + V_2 (\Delta x)_2 \dots \dots \dots [18]$$

The bending moment in shaft section 2 is now completely specified, and the slope θ_2 and the deflection y_2 at point 2 may be evalu-

ated by equations similar to Equations [15] and [16]. By repeating this process for successive sections, the bending moment and deflection diagrams for the remainder of the span may be calculated.

The equations for the n th section and point are listed as follows

$$V_n = V_{n-1} + m_{n-1} \omega^2 y_{n-1} \dots \dots \dots [19]$$

$$M_n = M_{n-1} + V_n (\Delta x)_n \dots \dots \dots [20]$$

$$\theta_n = \beta_n \left[\frac{M_{n-1}}{2} + \frac{M_n}{2} \right] + \theta_{n-1} \dots \dots \dots [21]$$

$$y_n = \beta_n \left[\frac{M_{n-1}}{3} + \frac{M_n}{6} \right] (\Delta x)_n + \theta_{n-1} (\Delta x)_n + y_{n-1} \dots [22]$$

where

$$\beta_n = \text{flexibility constant} = \left(\frac{\Delta x}{EI} \right)$$

It is convenient in carrying out these calculations in tabular form to introduce two auxiliary quantities; let

$$M_n' = \frac{M_{n-1}}{3} + \frac{M_n}{6} \dots \dots \dots [23]$$

$$M_n'' = \frac{M_{n-1}}{6} + \frac{M_n}{3} \dots \dots \dots [24]$$

Equations [21] and [22] may be expressed in terms of these auxiliary quantities as follows

$$\theta_n = \sum_{n=1}^n [\beta_n M_n' + \beta_n M_n''] + \theta_0 \dots \dots [25]$$

TABLE 1 SAMPLE CALCULATION AT ASSUMED SPEED OF 5000 RPM
($\omega = 523.6$ radians per sec, for span 1 of rotor shown in Fig. 2.)

	①	②	③	④	⑤	⑥	⑦	⑧	⑨	⑩	⑪	⑫	⑬	⑭	⑮	⑯	⑰	⑱
n	ΔV	V	ΔX	ΔM	M	$\frac{1}{3} M$	$\frac{1}{6} M$	M'	$\beta \cdot 10^3$	$\beta M'$	$\frac{\Delta y}{\Delta x}$	ΔX	$\Delta y'$	$\Delta y''$	y	$m \omega^2$	θ	$A \cdot \theta^2 \cdot m$
0	0	7,000			0	0	0	0							0	880	0	0
1	.0018	1,000	4,063	4,063	4,063	1,354	677	1,354	3.80	5.15	2.57	4,063	10.43	0	10,43	1760		1
2	.0176	1,001.8	4,063	4,067	8,133	2,711	1,355	3,388	3.80	12.87	16.01	4,063	73.2	0	83.6	2100		2
3	.2083	1,019.4	3,625	3,695	11,828	3,943	1,971	5,298	4.21	17.65	37.53	3,625	136.0	0	219.6	9490		3
4	1.311	1,227.7	5,188	6.37	18,20	6,067	3,033	8,038	4.21	18.44	53.50	5,188	277.6	0	497.2	26350		4
5	4.557	2,539	6,875	17.45	35,65	11,883	5,942	19,316	4.33	18.64	63.74	6,875	438.	0	935.	48700		5
6	2.988	7,096	6,000	42.6	78.2	26.07	13.04	24.32	4.37	19.34	65.32	6,000	392.0	0	1327.	22500		6
7	1.984	10,084	4,250	42.9	121.1	40.37	20.18	52.41	4.37	20.29	112.3	4,250	477.	0	1804.	10990		7
8	2.258	12,068	1,000	12.07	133.2	44.40	22.20	64.58	4.37	21.27	165.9	1,000	166.0	0	1970.	11460		8
9	1.203	14,326	6,125	87.7	220.9	73.63	36.82	95.83	4.37	22.6	319.2	6,125	1355.	0	3925.	3065		9
10	1.158	15,529	2,375	36.88	257.8	85.93	42.96	116.53	4.37	23.6	620.8	2,375	1475.	0	5400.	2145		10
11		16,687	3,688	61.5	319.3	106.43	53.22	133.15	4.37	24.6	906.2	3,688	3342.	0	8742.		1075.2	11
0	0	0			0	0	0	0							0	880	0	0
1	.7150	7,150	4,063	2,905	0	0	0	4840	3.80	14.64	.00184	4,063	.007	4,063	4,063	1760		1
2	.17080	24230	3,625	87800	29030	9680	4840	3680	3.80	14.64	.00348	3,625	.035	3,625	8,133	2100		2
3	.11,900	136,130	5,188	706,000	116,850	38950	19480	43790	4.21	17.65	.00622	5,188	.193	5,188	11,793	9490		3
4	453,000	589,100	6,875	4059,000	822,800	274,300	137,150	1,084,500	4.21	18.44	.01331	6,875	.532	6,875	17,174	26350		4
5	1,198,000	1,787,100	6,000	10,720,000	4,872,500	1,629,300	812,150	1,751,500	4.33	18.64	.02973	6,000	6.00	6,000	24,581	48700		5
6	702,000	2,489,100	4,250	10,580,000	5,553,000	1,858,000	929,000	2,084,500	4.37	19.34	.05099	4,250	4.597	4,250	31,187	22500		6
7	440,000	2,929,100	6,000	2,929,000	26,173,000	8,724,000	4,362,000	3,374,000	4.37	20.29	.07749	6,000	6.00	6,000	39,984	10990		7
8	455,000	3,384,100	6,125	2,918,000	29,020,000	9,701,000	4,850,000	4,061,000	4.37	21.27	.1070	6,125	6.125	6,125	43,190	11460		8
9	1,203	4,589,100	2,375	2,918,000	30,223,000	10,076,000	5,038,000	4,248,000	4.37	22.6	.14222	2,375	2.375	2,375	83,639	3065		9
10	1,158	5,747,100	3,688	2,918,000	31,426,000	10,404,000	5,202,000	4,582,000	4.37	23.6	.18935	3,688	3.688	3,688	115,560	2145		10
11		7,005,100	4,063	2,918,000	32,714,000	10,810,000	5,405,000	4,921,000	4.37	24.6	.24806	4,063	4.063	4,063	159,000		23,806	11

received after the close of the regular meeting of the Society.
understood as individual expressions of the Society.

$$y_n = \left\{ \beta_n M_n' + \sum_{n=1}^{n-1} [\beta_n M_n' + \beta_n M_n''] \right\} (\Delta x)_n + \theta_0 (\Delta x)_n + y_{n-1} \dots \dots \dots [26]$$

The form shown in Table 1 involves the use of Equations [19], [20], [25], and [26], together with the equations for the following auxiliary quantities:

$$(\Delta V)_n = m_n \omega^2 y_n \dots \dots \dots [27]$$

$$(\Delta M)_n = V_n (\Delta x)_n \dots \dots \dots [28]$$

$$(\Delta y')_n = \left\{ \beta_n M_n' + \sum_{n=1}^{n-1} [\beta_n M_n' + \beta_n M_n''] \right\} (\Delta x)_n \dots \dots [29]$$

$$(\Delta y'')_n = \theta_0 (\Delta x)_n \dots \dots \dots [30]$$

$$(\Delta y)_n = (\Delta y')_n + (\Delta y'')_n = y_n - y_{n-1} \dots \dots [31]$$

From the foregoing equations, it can be demonstrated that the shearing force, bending moment, slope, and deflection at any point in the span will be linear functions of the four assumed quantities at the left-hand end of the span, i.e., at point 0. Hence, the deflection, for example, at point *n* may be expressed by the following equation

$$y_n = A_n V_0 + B_n M_0 + C_n \theta_0 + D_n y_0 \dots \dots [32]$$

where *A_n*, *B_n*, *C_n*, and *D_n* represent numerical coefficients which may be determined by using the tabular form. Actually it is not necessary to determine all four coefficients. Since two boundary conditions must always be known at the end of the system from which the calculations originate, two of the terms in Equation [32] can be eliminated. Thus only two coefficients need to be evaluated and this is done in two parts on the tabular form.

The boundary conditions at the left-hand end of the system may be specified in general form as follows

$$\star \left(K y_0 = -V_0 \right) \dots \dots \dots [33]$$

$$C \theta_0 = M_0 \dots \dots \dots [34]$$

The minus sign in Equation [33] arises from the conventions employed. Terms *K* and *C* are stiffness constants which specify the elastic restraint exerted on the shaft by the supporting bearing. It is assumed that these stiffness constants are symmetrical, i.e., of the same magnitude for all directions normal to the shaft.

The boundary conditions take the following form for certain limiting cases:

Fixed End. The bearing is infinitely stiff against both displacement and rotation or tilting of the shaft, i.e., *K* = *C* = ∞. Hence from Equations [33] and [34], the following conditions must apply if the shearing force and bending moment are to be finite: *y*₀ = 0 and *θ*₀ = 0.

Simply Supported End. The bearing is infinitely stiff against displacement but offers no restraint to tilting of the shaft, i.e., *K* = ∞, *C* = 0. Hence *y*₀ = 0 and *M*₀ = 0.

Free End. The shaft end is completely free, i.e., *K* = *C* = 0; hence *V*₀ = 0, and *M*₀ = 0.

The boundary conditions that apply at a common point between two spans of a multispan rotor are specified in the following manner: Let *k* denote the common point between span 1 and span 2. By reason of the continuity of the shaft

$$(\theta_k)_{span\ 2} = (\theta_k)_{span\ 1} \dots \dots \dots [35]$$

$$(y_k)_{span\ 2} = (y_k)_{span\ 1} \dots \dots \dots [36]$$

The bearing reactions are treated by equations similar to Equations [33] and [34]

$$K y_k = -[(V_k)_{span\ 2} - (V_k)_{span\ 1}] \dots \dots \dots [37]$$

$$C \theta_k = [(M_k)_{span\ 2} - (M_k)_{span\ 1}] \dots \dots \dots [38]$$

SAMPLE CALCULATION

The drawing of the rotor used for this calculation is given in Fig. 2. The rotor has two spans, span 1 being supported between two bearings, and span 2 being overhung. Also shown in Fig. 2 is a diagrammatic representation of the idealized system. This idealized system is obtained by dividing the shaft of the rotor into sections of constant diameter. The total mass existing within a given section is divided into two parts which are concentrated at the ends of the section, this division of mass being such that the center of gravity of the section mass remains unchanged. The flexibility constants are evaluated using the actual physical dimensions of the shaft sections. While this method of constructing the idealized system is somewhat arbitrary, it should be sufficiently accurate for all practical purposes provided enough sections are used.

In Table 1, the calculations for span 1 are given in tabular form for an assumed speed of 5000 rpm (*ω* = 523.6 radians per sec). The values for the section lengths *Δx*, disk masses *m*, and shaft-flexibility constants *β* for the idealized system, as shown in Fig. 2, are listed directly on the tabular form in the proper columns (the values of the masses being multiplied by *ω*² to give the inertia force constants *mω*²). In so far as the calculation is concerned, the rotor is completely specified by these three groups of quantities. (It is assumed that the disks on the rotor have negligible moment of inertia, i.e., there is no gyroscopic effect.)

The assumption is made that the shaft is simply supported in its bearings. From Equations [33] and [34], the following boundary conditions are obtained for the left-hand end of span 1 (point 0)

$$y_0 = 0$$

$$M_0 = 0$$

The shearing force *V*₀ and the slope of the deflection curve *θ*₀ are carried in the calculation as unknowns. On the tabular form this is done by making the calculation in two parts with the following initial conditions (note the encircled figures in Table 1),

$$I \left\{ \begin{matrix} V_0 = 1.000 \\ \theta_0 = y_0 = M_0 = 0 \end{matrix} \right. \quad II \left\{ \begin{matrix} V_0 = y_0 = M_0 = 0 \\ \theta_0 = 1.000 \end{matrix} \right.$$

With the initial conditions specified the calculation proceeds across the table from left to right, the figures on one horizontal line being completed before proceeding to the next line. Although the general equations given in the preceding section of the paper define all of the operations on the form, several features may need further explanation. Values pertaining to the mass points are entered on the horizontal lines. Values pertaining to the shaft sections are entered in the spaces between the lines. The auxiliary quantities *M'* and *M''* in column 8 are each obtained by adding together one value from column 6 and one value from column 7. The manner in which this addition is made is indicated by the arrows inserted on the form. The quantity $\left(\frac{\Delta y'}{\Delta x} \right)$ in column 11 is obtained by a summation of the values in column 10 proceeding from the top of the column down to but not including the second of the two values for the last section involved in the particular summation. The broken lines drawn on the form in columns 10 and 11 indicate the values involved in successive summations. The slope *θ* in column 17 is obtained by summing the values in column 10 from the top down to the point for which the slope is desired.

From the calculations in Table 1, the following equations are

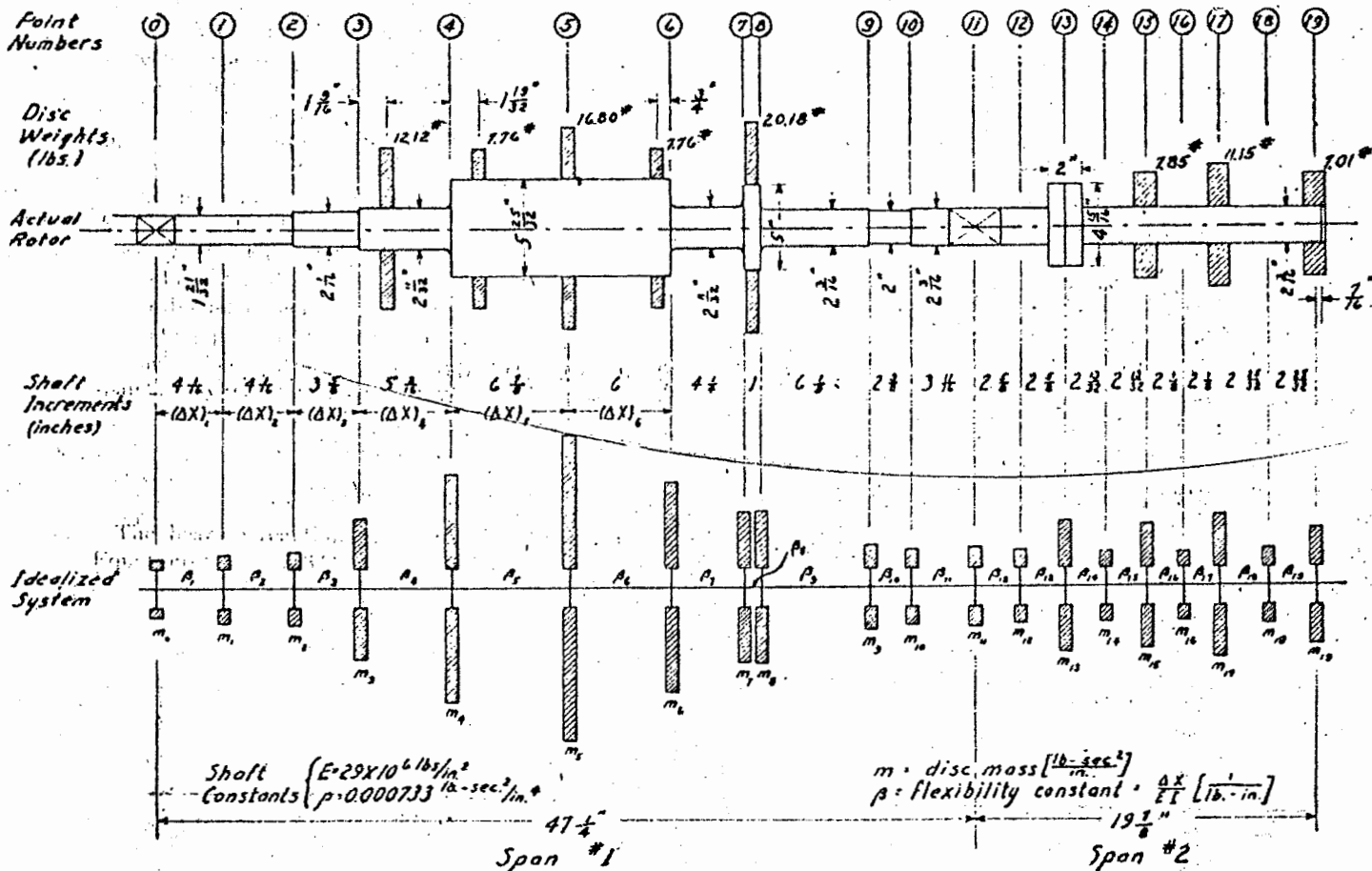


FIG. 2 ROTOR USED FOR SAMPLE CALCULATION

obtained for the slope, deflection, and bending moment at point 11 (the common point between span 1 and span 2)

$$\theta_{11} = 0.00016752 V_0 + 23.806 \theta_0 \dots \dots \dots [39]$$

$$y_{11} = 0.0008742 V_0 + 189.0 \theta_0 \dots \dots \dots [40]$$

$$M_{11} = 319.3 V_0 + 73,270,000 \theta_0 \dots \dots \dots [41]$$

From Equations [35] through [38], the following boundary conditions are obtained at point 11 (shaft simply supported in the bearing)

$$\begin{aligned} (\theta_{11})_{\text{span 2}} &= (\theta_{11})_{\text{span 1}} \\ (y_{11})_{\text{span 2}} &= (y_{11})_{\text{span 1}} = 0 \\ (M_{11})_{\text{span 2}} &= (M_{11})_{\text{span 1}} \end{aligned}$$

Placing y_{11} equal to zero in Equation [40] gives V_0 in terms of θ_0 . Hence V_0 may be eliminated from Equations [39] and [41]. Then by virtue of the foregoing boundary conditions, the following values apply to the initial point for span 2

$$\begin{aligned} \theta_{11} &= 0.561 \theta_0 \\ y_{11} &= 0 \\ M_{11} &= 4,240,000 \theta_0 \end{aligned}$$

Because of the unknown bearing reaction, the shearing force V_{11} for span 2 is not known. Hence the calculations for span 2 are made in terms of the two unknowns, V_{11} and θ_0 . On the tabular form this is done by making the calculations in two parts with the following initial conditions

$$\text{I } \begin{cases} V_{11} = 1.000 \\ \theta_{11} = y_{11} = M_{11} = 0 \end{cases} \quad \text{II } \begin{cases} V_{11} = y_{11} = 0 \\ M_{11} = 4,240,000 \\ \theta_{11} = 0.561 \end{cases}$$

The calculations for span 2 are carried out in the same manner

as for span 1. They have not been included in this paper because of space limitations. From these calculations the following equations are obtained for V_{20} , the shearing force at an infinitesimal distance beyond the point of attachment of the 19th disk, and M_{19} , the bending moment at point 19

$$V_{20} = 1.523 V_{11} + 688,400 \theta_0 \dots \dots \dots [42]$$

$$M_{19} = 21.469 V_{11} + 7,470,000 \theta_0 \dots \dots \dots [43]$$

Since point 19 represents the free end of the rotor, the following boundary conditions apply

$$\begin{aligned} V_{20} &= 0 \\ M_{19} &= 0 \end{aligned}$$

In general, only one of these conditions can be satisfied. Only if the assumed speed is exactly equal to a critical speed will both conditions be satisfied. Placing V_{20} equal to zero in Equation [42] and solving for M_{19} in terms of θ_0 in Equation [43] yields the following value for M_{19}

$$M_{19} = -2,230,000 \theta_0$$

Since M_{19} is not equal to zero, the assumed speed of 5000 rpm does not represent a critical speed. A series of calculations similar to the one just discussed have been made for this rotor at different assumed speeds. The values of M_{19} obtained from these calculations have been plotted against assumed speed in Fig. 3. In plotting these values of M_{19} , the slope θ_0 at the left-hand end of the rotor is arbitrarily placed equal to unity. (Any value may be assigned to θ_0 since, at a critical speed, the rotor is in a state of indifferent equilibrium.) The first three values of speed required to make M_{19} equal to zero are as follows:

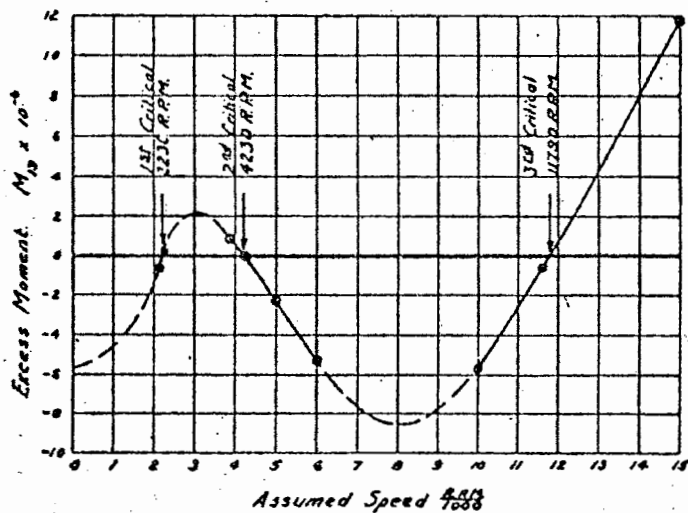


FIG. 3 PLOT OF EXCESS BENDING MOMENT VERSUS ASSUMED SPEED

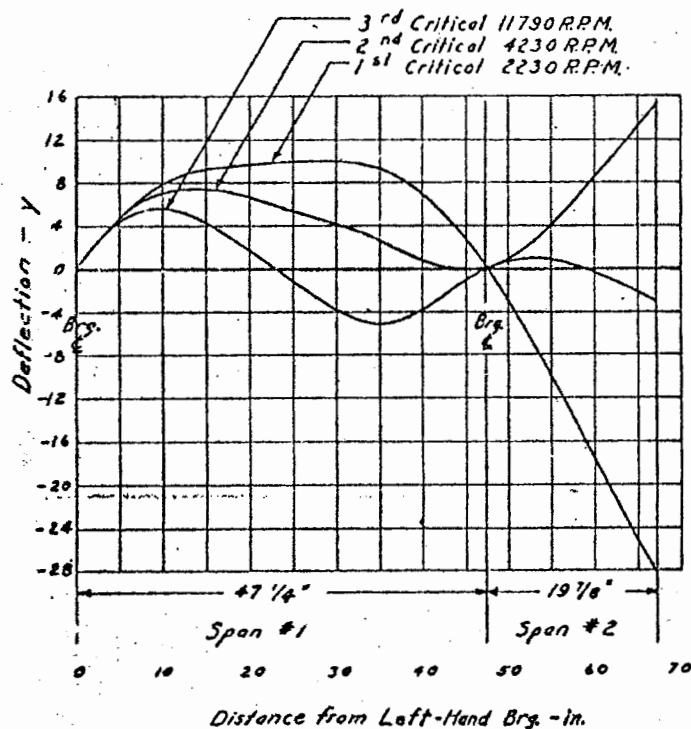


FIG. 4 DEFLECTION CURVES FOR FIRST, SECOND, AND THIRD CRITICAL SPEEDS

- Critical speed 1 = 2230 rpm
- Critical speed 2 = 4230 rpm
- Critical speed 3 = 11,790 rpm

The deflection diagram may be readily plotted for any assumed speed, since an equation of the form of Equation [40] may be obtained from the tabular calculation for every point along the rotor. The deflection curves for the first three critical speeds have been plotted in Fig. 4.

EFFECT OF MASS MOMENT OF INERTIA OF DISKS

Assume that values of mass moment of inertia, both polar and diametral, have been assigned to the disks of the idealized system. The effect of the mass moment of inertia may be readily taken into account on the tabular form. It is necessary, however, to differentiate between the nonrotating and rotating cases.

Nonrotating Case. For a rotor which is vibrating in a trans-

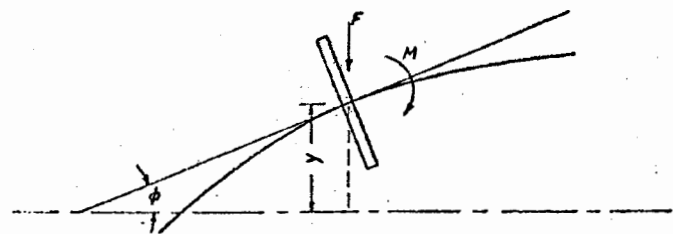


FIG. 5

verse plane at a natural frequency, a rotary inertia effect is involved. Consider a disk on a vibrating shaft at the instant of maximum amplitude, as shown in Fig. 5. Let the deflection of the disk center of gravity be denoted by y , the angle of rotation by ϕ , and the frequency of vibration by ω . The force F and the moment M which must be exerted on the disk with respect to its center of gravity are

$$F = m\omega^2 y \dots \dots \dots [44]$$

$$M = B\omega^2 \phi \dots \dots \dots [45]$$

where B is the mass moment of inertia of the disk about an axis through the center of gravity and normal to the axis of symmetry.

The force and the moment which the disk exerts on the shaft will have magnitudes equal to the foregoing values, but will have directions opposite to those shown in Fig. 5.

Equation [44] requires that there be a change in shearing force in the shaft at the point of attachment of the disk proportional to the deflection, the proportionality factor being $m\omega^2$. This has already been incorporated in the calculation procedure. Equation [45] requires that there be a change in bending moment at the point of attachment of the disk proportional to the angle ϕ , the proportionality factor being $B\omega^2$. In terms of the notation employed on the tabular form Equation [45] becomes

$$\Delta M = -B\omega^2 \theta \dots \dots \dots [46]$$

where the slope θ has been substituted for the angle ϕ . (This is permissible for small angles.)

Rotating Case. For a rotor which is whirling at a critical speed, a gyroscopic effect is involved. Consider a balanced disk, as shown in Fig. 6, the center of gravity of which is whirling in a circular path of radius y at a speed ω . Let the axis of the disk make a constant angle ϕ with the rotation axis. Assume that there is no rotation of the disk relative to the rotating plane formed by the disk axis and the rotation axis. This means that a point Q , for example, which is the outside point on the periphery of the disk will remain the outside point.

The components of rotation about the axes a and b are $\omega \cos \phi$ and $\omega \sin \phi$, respectively. Since axes a and b are principal axes of inertia for the disk, the components of angular momentum H_a and H_b are given by the following formulas

$$H_a = A\omega \cos \phi$$

$$H_b = B\omega \sin \phi$$

where A and B are the mass moments of inertia of the disk about axes a and b , respectively.

The moment which must act on the disk about the center of gravity to sustain the prescribed motion is equal to the time rate of change of the resultant angular momentum H

$$M = \frac{dH}{dt} = H_y \omega \dots \dots \dots [47]$$

where H_y is the component of H normal to the axis of rotation

$$H_y = H_a \sin \phi - H_b \cos \phi$$

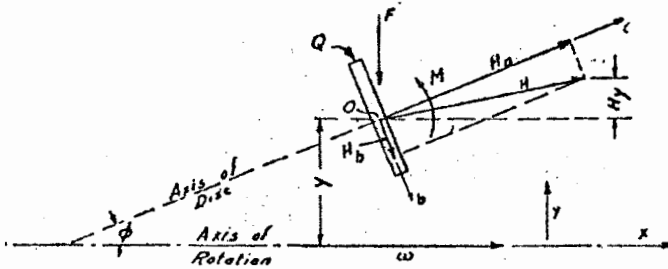


FIG. 6

or

$$H_y = (A - B)\omega \sin \phi \cos \phi \dots [48]$$

Substituting Equation [48] in Equation [47], and placing $\sin \phi = \phi$ and $\cos \phi = 1$ (permissible for small angles) gives

$$M = (A - B)\omega^2 \phi \dots [49]$$

The direction of this moment is in the direction of the change of momentum, as indicated in Fig. 6. It will be noted that the direction of this moment is opposite to that shown in Fig. 5, for the nonrotating case. In addition to the moment M , given by Equation [49], a centripetal force F , as given by Equation [44], is required to maintain the prescribed motion.

The force and the moment which the disk exerts on the shaft will be equal in magnitude to F and M in Fig. 6, but opposite in direction.

Expressing Equation [49] in terms of the notation on the tabular form gives the expression

$$\Delta M = (A - B)\omega^2 \phi \dots [50]$$

If the disks of the idealized system have appreciable mass moment of inertia, then the bending-moment diagram, shown in Fig. 1, must be modified as indicated in Fig. 7. Because of the finite change in bending moment which occurs at each point according to Equation [50], there will be two values of bending moment at each point. Thus in Fig. 7, M_{1L} signifies the bending moment at an infinitesimal distance to the left of the point of attachment of the disk and M_{1R} the bending moment at an infinitesimal distance to the right.

The last two columns on the form, Table 1, have been added so that the effect of the mass moment of inertia of the disks may be incorporated into the calculation. The heading of column 18 applies to the rotating case. If a nonrotating case is to be handled, the symbol A should be deleted from the heading, according to Equation [46]. The values of ΔM obtained by Equation [46] or Equation [50] are tabulated in column 4 of the form, the values being entered on the horizontal lines. (The values of ΔM due to the shearing force in the shaft sections are entered in the space between the lines.) This dual set of values for ΔM gives rise to two values of bending moment at each point in column 5. The first value is entered just above the horizontal line bearing the point number, and the second value just below. The rest of the calculation is then the same as the sample shown in Table 1.

The mass moments of inertia A and B for a flat solid disk are given by the following equations

$$A = \frac{\pi \rho h D^4}{32} \dots [51]$$

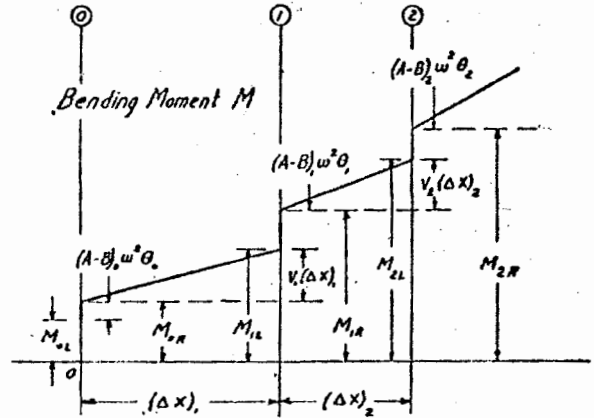


FIG. 7 BENDING-MOMENT DIAGRAM FOR SYSTEM OF FIG. 1, WHERE THE DISKS HAVE APPRECIABLE MASS MOMENT OF INERTIA

$$B = \frac{\pi \rho h D^4}{64} \left[1 + \frac{4}{3} \left(\frac{h}{D} \right)^2 \right] \dots [52]$$

If the thickness h of the disk is small compared to the diameter D , then $A \cong 2B$, and the proportionality factors between moment and slope in Equations [46] and [50] become equal in magnitude but opposite in sign.

For the nonrotating case, the natural frequencies obtained by neglecting the mass moment of inertia are decreased if the effect of the mass moment of inertia is considered. For the rotating case, the critical speeds are increased by taking into account the mass moment of inertia provided that $A > B$.

CONCLUSIONS

The tabular-calculation method presented in this paper gives an exact solution for the critical speeds of the idealized system. Hence the accuracy of the method in so far as an actual rotor is concerned depends entirely on how closely the idealized system and the idealized boundary conditions represent the actual rotor and its bearings.

ACKNOWLEDGMENT

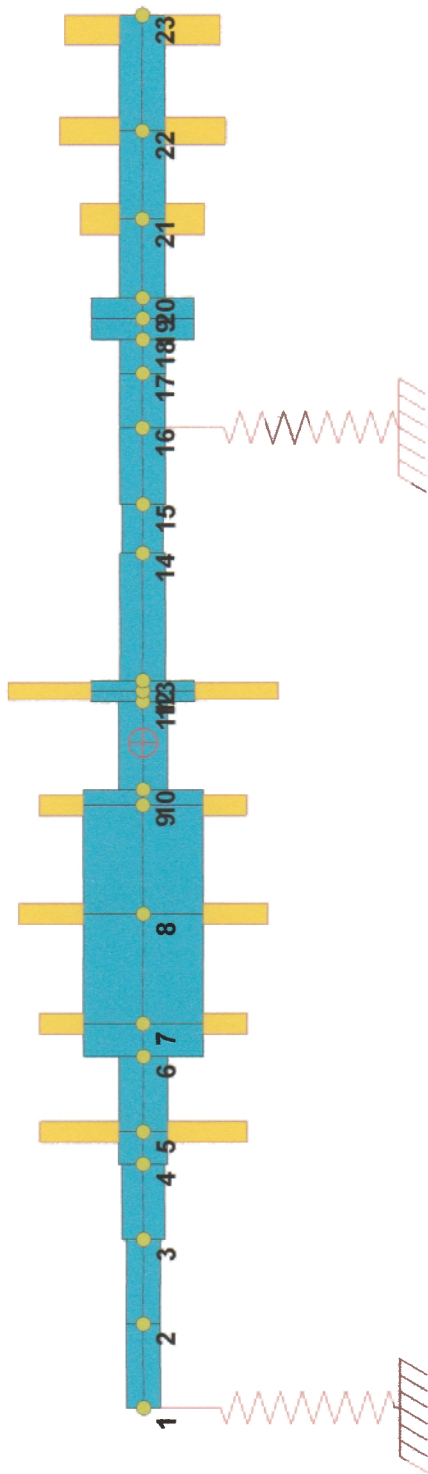
The author wishes to express his appreciation to Dr. H. Poritsky of the Engineering General Division of the General Electric Company, Schenectady, N. Y., for originally outlining the general method of attacking this problem and for his suggestions and comments.

BIBLIOGRAPHY

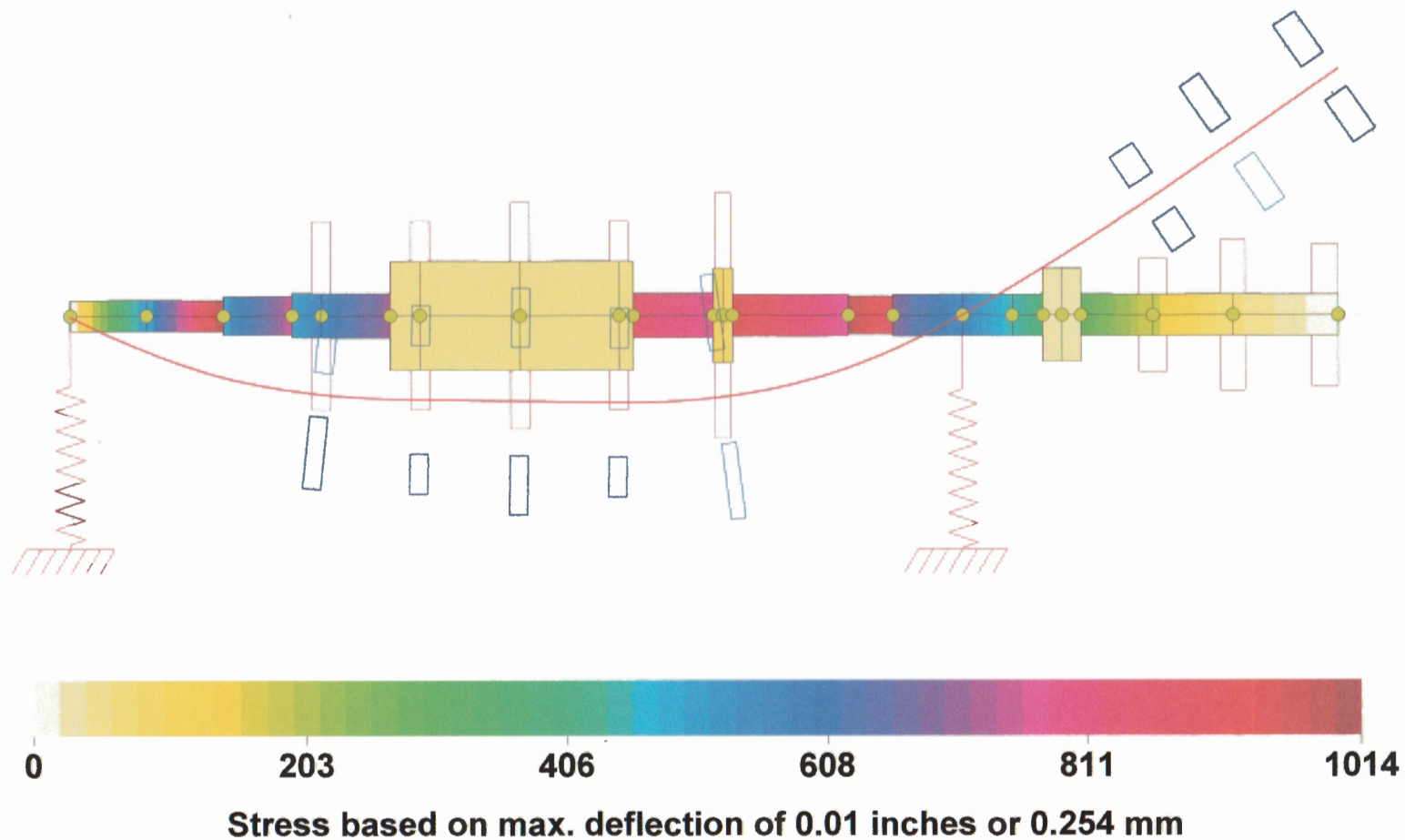
- 1 "Mechanical Vibrations," by J. P. Den Hartog, McGraw-Hill Book Company, Inc., New York, N. Y., 1940, pp. 194-196.
- 2 "On the Strength of Shafting When Exposed Both to Torsion and End Thrust," by A. G. Greenhill, Proceedings of The Institution of Mechanical Engineers, 1883, pp. 182-225.
- 3 "On the Whirling and Vibration of Shafts," by S. Dunkerley, Philosophical Transactions of the Royal Society of London, series A, vol. 185, 1894, pp. 279-360.
- 4 Reference (1), pp. 222-237.
- 5 "Strength of Materials, Part I," by S. Timoshenko, D. Van Nostrand Company, Inc., New York, N. Y., 1940, pp. 72-74.
- 6 "A New Method of Calculating Natural Modes of Uncoupled Bending Vibration of Airplane Wings and Other Types of Beams," by N. O. Myklestad, Journal of the Aeronautical Sciences, vol. 11, no. 2, April, 1944, pp. 153-162.

PROHL ROTOR - Linear Bearings

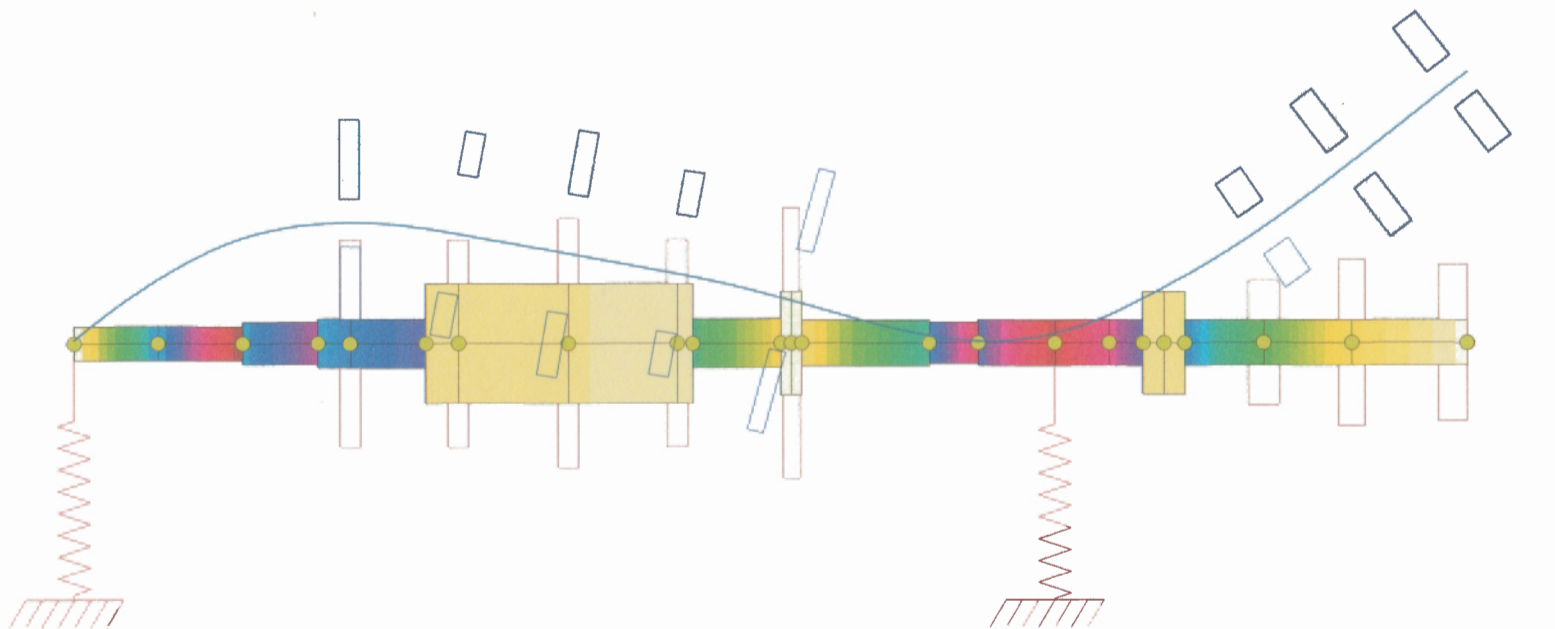
$K_b = 1.0E6 \text{ Lb/IN}$



PROHL ROTOR - Linear Bearings
 $K_b = 1.0E6$ Lb/IN
Critical Speed Mode Shape, Mode No.= 1
Spin/Whirl Ratio = 1, Stiffness: Kxx
Critical Speed = 2212 rpm = 36.87 Hz



PROHL ROTOR - Linear Bearings
 $K_b = 1.0E6$ Lb/IN
Critical Speed Mode Shape, Mode No.= 2
Spin/Whirl Ratio = 1, Stiffness: Kxx
Critical Speed = 4276 rpm = 71.26 Hz



0

427

854

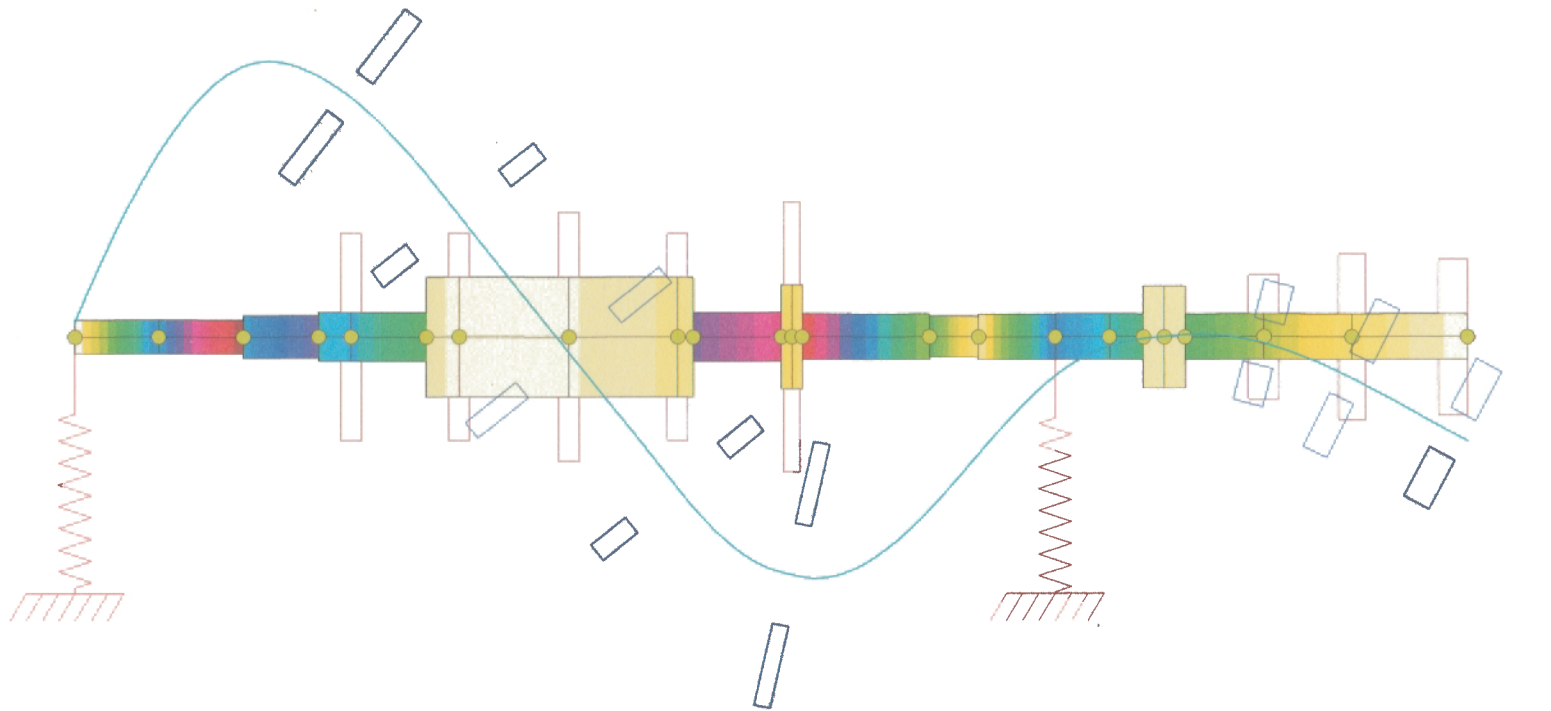
1281

1708

2134

Stress based on max. deflection of 0.01 inches or 0.254 mm

PROHL ROTOR - Linear Bearings
 $K_b = 1.0E6$ Lb/IN
Critical Speed Mode Shape, Mode No.= 3
Spin/Whirl Ratio = 1, Stiffness: Kxx
Critical Speed = 12392 rpm = 206.53 Hz



0 1661 3322 4983 6644 8305

Stress based on max. deflection of 0.01 inches or 0.254 mm